Society of Petroleum Engineers

SPE-224378-MS

Automatic Depth Alignment of High-Resolution Magnetic Flux Leakage Data to Detect Corrosion in Downhole Casing Using Machine Learning

Shejuti Silvia, Ted Furlong, and Torben Goetzche, Baker Hughes, Houston, Texas, US

This paper was prepared for presentation at the SPE Oklahoma City Oil and Gas Symposium, held in Oklahoma City, Oklahoma, USA, 14-18 April 2025.

Abstract

Periodically monitoring well casing and tubing integrity is essential for making timely decision for well intervention to safely operate oil and gas wells. Magnetic flux leakage (MFL) inspection tools are most used in downhole casing inspections. Due to different positions of the sensors on the inspection tool, the MFL data measured by the sensors are misaligned. These data need to be aligned before they can be used for further analysis. Oil and gas operators rely on human experts to align and analyze these data to assess corrosion defects in casing. This analysis done by different individuals at different times, using different data processing tools supporting their interpretation, often leads to inconsistent risk evaluation. In this paper, we demonstrate results from a machine learning (ML) based approach that automatically aligns multiaxial MFL inspection data, enabling consistent and accurate identification of corrosion defects in well casing.

High resolution MFL casing inspection tool used in this study consists of dual inspection modules – upper and lower. Each inspection module houses 48 tri-axial flux leakage (FL) sensors and 48 discriminator (DIS) sensors. Data from casing inspection included – 1) Memory data: high-resolution flux leakage data from FL and DIS sensors, acceleration data stored in tool's memory, 2) Monitoring data: low-resolution flux leakage data from FL and DIS sensors, acceleration data, winch speed, and tool depth stored in the surface data acquisition system. We applied a pattern recognition technique to identify the casing joint collar signatures in flux leakage data. Then we used Genetic Algorithm (GA) to align collars identified in – 1) upper and lower modules data, 2) memory and monitoring data and 3) monitoring data and previous inspections reports with physical depth of collars. The final output of our algorithm is the aligned high-resolution MFL data from memory, associated with physical depth, suitable for corrosion defect evaluation.

We used historical casing inspections data, reports and gamma-ray and neutron correlation logs from a vertical well in North America (Well 1) to demonstrate results from our algorithm. Accuracy of the depth alignment of the high-resolution MFL data was evaluated using the average Euclidean distance (mm) between the casing joint collars in memory, monitoring data and previous inspections reports. Our proposed algorithm outperformed the existing methods by achieving less than 50 mm or 2 inches misalignment between 90% of the collars in the upper and lower modules. It also achieved reasonable alignment between 75% of the collars identified in monitoring and memory data, as well as, between previous reports and in the memory data.

MFL casing inspection data are noisy due to vertical and rotational movement of the tool inside the well casing. These data also include missing and erroneous data from sensor failures. The proposed method is robust enough to perform well under such circumstances. Traditional methods rely on human experts to manually align MFL data for detecting corrosion in casing, leading to inconsistent risk evaluation of trends. The main contribution of this paper is the automatic depth alignment of the high-resolution MFL data, by analyzing the historical inspection reports. This enables higher accuracy and consistency in assessing corrosion progression in well casing over time.

Introduction

The high resolution MFL casing inspection system discussed in this study is illustrated in Figure 1. It consists of a high resolution MFL inspection tool, wireline logging unit controlling the inspection tool, moving it up and down the well casing; and the surface data accusation system recording data collected by the MFL inspection tool downhole [Vogtsberger et. al. 2005]. As showed in Figure 1, the high-resolution MFL casing inspection tool comprises of upper and lower inspection modules, each housing 48 tri-axial flux leakage sensors1 (FL) and 48 discriminator (DIS) sensors, covering 100% of the casing wall circumference. [Veanch et. al. 2005, Fickert et. al. 2005, Vogtsberger et. al. 2005, Barolak et. al. 2009].

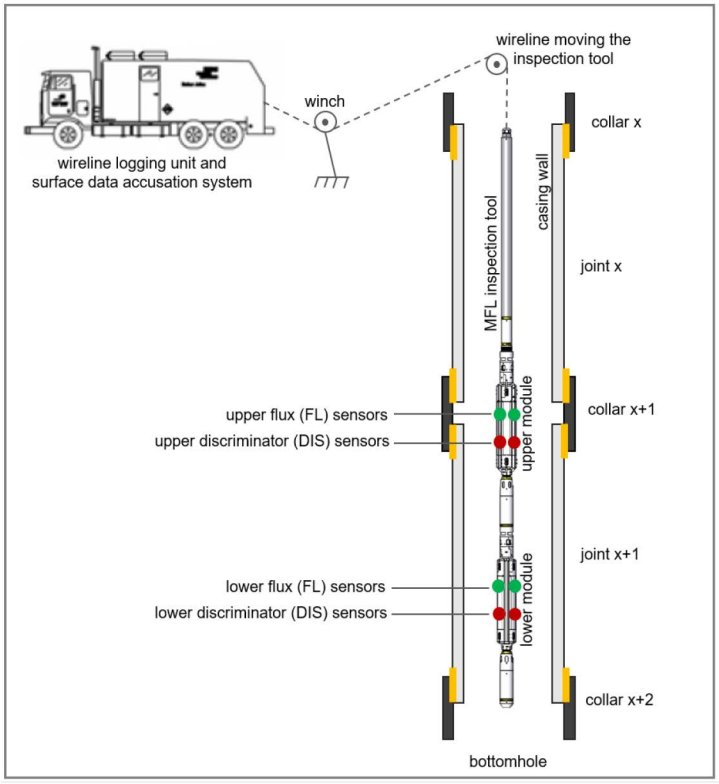

Figure 1—High resolution MFL inspection system for well tubing and casing integrity evaluation.

As illustrated in Figure 2(a), the FL sensors are deployed within a permanent magnet circuit that produces high density of magnetic flux within the casing wall. Hardware, such as the metal collars at the casing joints, centralizers and scratchers, as well as corrosion defects on the casing wall cause flux perturbations ("leakage") that are measured by the FL sensors on the inspection modules [Vogtsberger et. al. 2005, El Sherbeny et. al. 2015, Foster et. al. 2015].

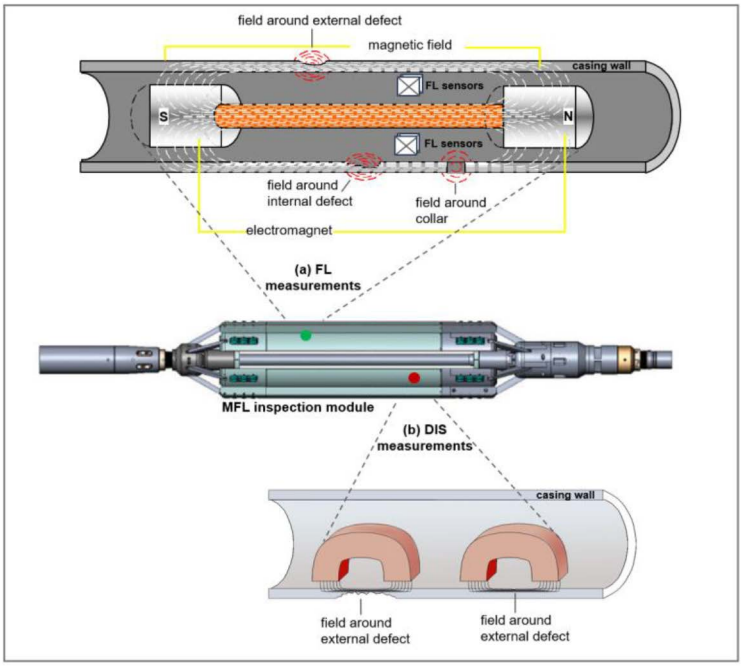

Figure 2—(a) FL sensors deployed with permanent magnet circuit producing a very high magnetic flux density within the casing wall; (b) DIS sensors deployed within a weak magnetic field producing flux density only within the inner surface of the casing wall.

However, the FL sensors cannot differentiate between internal and external hardware and defects. Therefore, as illustrated in Figure 2(b), the DIS sensors are deployed within a weak magnetic field that produces flux density only within the inner surface of the casing wall. Thus, the external hardware or defects do not perturb this magnetic flux path. Only the internal hardware or defects on the casing wall will perturb this weak magnetic flux path. Therefore, the DIS sensors measurements are used to differentiate between the internal and external defects or hardware in casing [Vogtsberger et. al. 2005, El Sherbeny et. al. 2015, Foster et. al. 2015]. Figure 3 shows flux leakage measurements from upper and lower FL and DIS sensors around two casing collars.

Oil and gas operators rely on human experts to analyze the high-resolution MFL casing inspection data periodically to monitor their well integrity. Operators are particularly interested in monitoring progression of corrosion related defects in well casing and tubing to take timely decision for remedial action or well abandonment. To evaluate corrosion progression and overall, well integrity, the experts have to analyze the recent casing inspection data of a well, alongside its previous inspection data. Using the existing software with many manual and semi-automated workflows, it takes an expert around 30 hours to analyze single casing inspection data. This significantly limits the number of wells operators can evaluate to ensure their safe operation. In this paper, we demonstrate development of a new algorithm to automate the first step of analyzing the casing inspection data – identifying and aligning (depth of) casing collar signatures in flux leakage data from FL and DIS sensors in upper and lower inspection modules. Proper alignment of these sensor measurements enables accurate detection of corrosion defects in casing inspection data. Accurate identification of collars also helps differentiating collar signatures from corrosion defect signatures in flux leakage data. Figure 3 shows misaligned collar signatures in flux leakage data from FL and DIS sensors in upper and lower inspection modules.

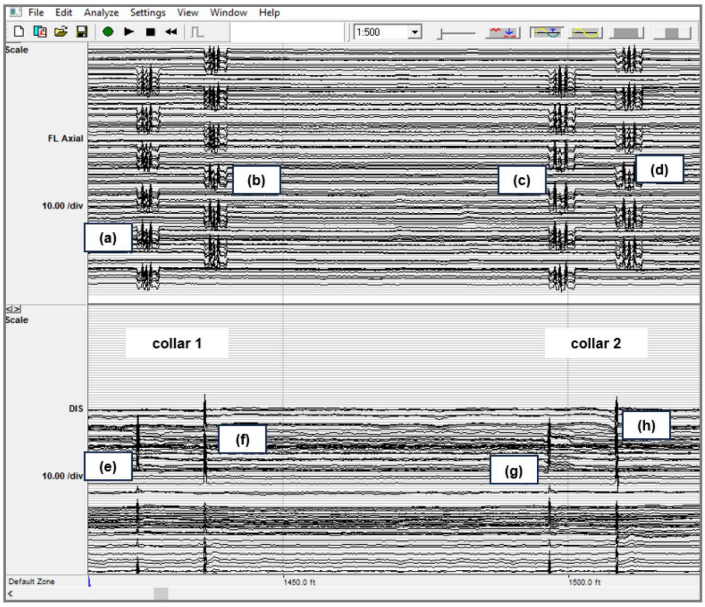

Figure 3—FL & DIS measurements around casing collars in the upper and lower inspection modules during up-pass log (MFL tool moving from bottomhole to the surface). (a) Lower FL sensor response around collar 1; (b) Upper FL sensor response around collar 1; (c) Lower FL sensor response around collar 2; (d) Upper FL sensor response around collar 2; (e) Lower DIS sensor response around collar 1; (f) Upper DIS sensor response around collar 1; (g) Lower DIS sensor response around collar 2; (h) Upper DIS sensor response around collar 2.

Data Description

For this case study, data listed in Table 1 were collected from 200 casing inspections in North America. Most of these data include reports from past several years of casing inspections of the same well. Equipment data from the surface accusation system were used to identify number of sensors and depth offset between each sensor measurement in upper and lower inspection modules.

Table 1—Data collected for 200 casing inspections in North America

	Source	Type of Data	Data
(a)	Surface accusation system	Job data, well data, casing data, equipment data, low resolution monitoring data	Job details, well name, location, operator name, casing specifications, MFL inspection tool model and configuration data, winch speed, tool depth, low resolution accelerometer and flux leakage data sent from the MFL tool downhole
(b)	MFL tool memory data	High resolution memory data	High resolution accelerometer and flux leakage data recorded in MFL inspection tool's memory
(c)	Previous inspection reports	Previous casing joint interpretation summary/ risk evaluation	Number of casing joints, other hardware on casing, flange, collars, corrosion defects along with their depth reported in previous inspections
(d)	Gamma-ray and neutron correlations logs	Official casing tally records from operators	Actual physical depth of casing joints

Inspection data logged in the surface accusation system, a. k. a. the monitoring data include low-resolution (5 ms sampling rate) winch speed, tool depth, tri-axial accelerometer data, along with flux leakage data from 48 axial, radial and circumferential FL sensors (as showed in Figure 4) and 48 DIS sensors. Inspection data logged in the MFL tool's memory include 320 Hz high-resolution flux leakage data for the same channels as the monitoring file. However, the memory data do not record any speed and depth information. Therefore, though the high-resolution MFL data in memory are more useful for detecting collar and defect signatures,

we are not able to use it until we estimate its depth from the accelerometer data in memory and the winch speed and depth from the monitoring data. The algorithm to estimate depth in high-resolution MFL data is discussed in detail in the next section.

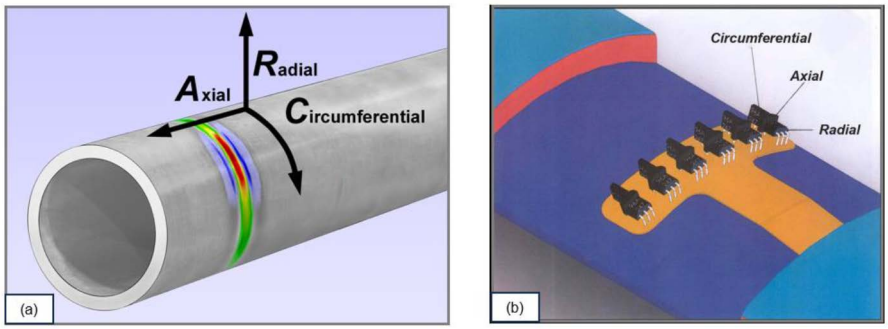

Figure 4—(a) FL sensors on MFL inspection tool is designed to acquire 3 axial components of the magnetic flux leakage created by metal collars and defects on casing wall; (b) Tri-axial FL sensors placed on the MFL inspection tool.

Methodology

To leverage the high-resolution MFL inspection data for improved detection and depth estimation of corrosion defects and other hardware features, such casing joint collars, we propose the algorithm in Table 2. Our algorithm uses combination of pattern recognition techniques and Genetic Algorithm minimization routines to first align collars between memory and monitoring data. And then estimate depth my matching the memory and monitoring collars with the physical depth of casing collars from previous report. Unlike the existing analytic tools, our proposed algorithm requires no manual intervention to match the MFL data with physical depth of well casing.

Table 2—Proposed algorithm for automatic depth alignment of high-resolution magnetic flux leakage data

	Algorithm 1: Depth alignment of high-resolution MFL data
1	Centering and denoising flux leakage data
2	Align monitoring data using tool configuration offsets
3	Design custom filters to detect collars in flux leakage data
4	Detect collars in monitoring and memory data
5	Estimate tool speed in high-res. memory data using monitoring winch speed and memory accelerometer data
6	Estimate tool depth in high-res. memory data from tool speed
7	GA minimizer 1: Align memory collars using tool depth
8	GA minimizer 2: Finetune tool depth by aligning memory collars with monitoring collars
9	GA minimizer 3: Finetune tool depth by aligning monitoring and memory collar depth with previous inspection report

The next section describes the algorithm in more detail with results from Well 1 casing inspection.

Results and Discussion

The step-by-step process of our algorithm, along with results are described as below.

Centering and Denoising Flux Leakage Data:

The accelerometer data and the flux leakage data from MFL inspection tool are noisy and often skewed due to tool calibration issues. To prepare the data for detecting casing collars and defects effectively, we first removed sensor errors and outliers, centered each sensor signal around ‘0’, then applied a lowpass filter to reduce the noise. Resulting pre-processed data are showed in Figure 5 below.

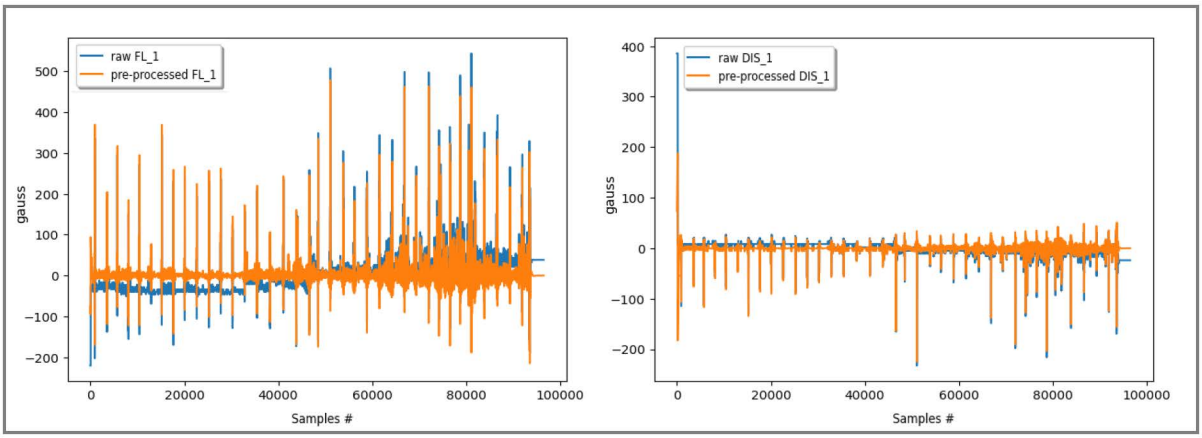

Figure 5—Raw vs. pre-processed flux leakage data from FL 1 (left) and DIS 1 (right) sensor.

After pre-processing the sensor data in both monitoring and memory files using this method, we applied our algorithm to align the sensor data in monitoring file as described below.

Align Monitoring Data

As showed in Figure 1, due to the physical distance between the upper and the lower inspection modules in the MFL tool, the flux leakage sensor timeseries from these two modules are misaligned; in other words, have lags or leads between them. To detect collars and defects, these flux leakage timeseries need to be aligned first. We applied a two-step solution to align monitoring sensor timeseries as described below.

Apply Tool Configuration Offsets. The distance (in mm) between the upper and lower module sensors were retrieved from the tool configuration data stored in the MFL tool surface acquisition software. These depth offsets were applied on each sensor timeseries in the monitoring file. Figure 6(a) shows 2 FL and 2 DIS sensors timeseries from monitoring file, before (left) and after (right) applying the offsets. The red arrows on the left figure in Figure 6(a) highlights the misalignment of the same collar signatures in flux leakage data from 4 different sensors. The red lines on the right figure in the Figure 6(a) highlights the aligned collars in these sensor data, after applying the depth offsets from toll configuration.

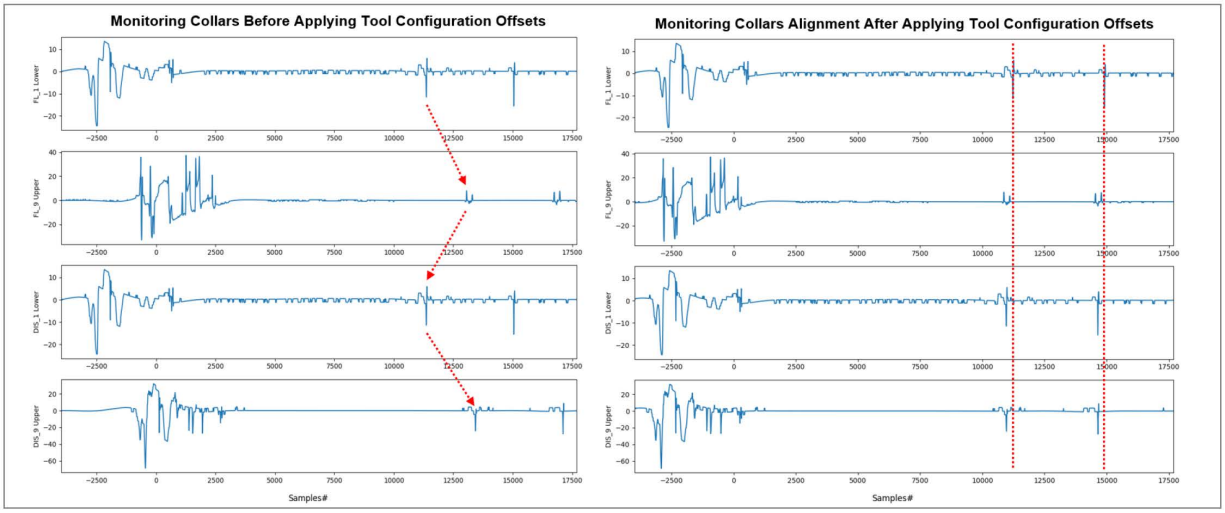

Figure 6(a)—Misaligned flux leakage timeseries before (left) and aligned flux leakage data after (right) applying the tool configuration offsets

Apply Cross Correlation Coefficient. As showed in the right of Figure 6(b), after applying the tool configuration offsets, there are still small misalignments between each sensor timeseries. This could be due to slight distortion in sensor positions on the tool. To further align the data, we have calculated the correlation coefficients and lags between each pair of FL 1 sensor timeseries with the rest of the 95 sensor timeseries in the monitoring file. The lag value associated with the greatest correlation coefficient was used as sample shifts to align each sensor timeseries with FL 1. Figure 6(b) shows 2 FL and 2 DIS sensor timeseries from monitoring file, before (left) and after (right) applying the sample shifts from the cross-correlation analysis. The right figure in 6 (b) shows perfect alignment between collar signatures from these 4 sensors.

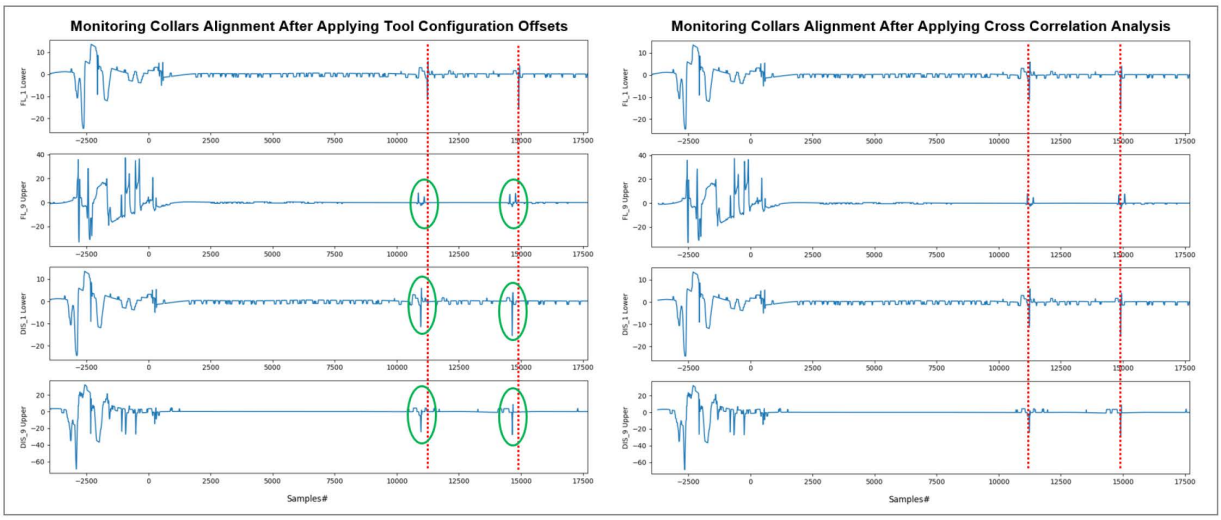

Figure 6(b)—Slightly misaligned flux leakage timeseries before (left) and completely aligned flux leakage data after (right) applying the sample shifts from cross correlation analysis.

Next, the aligned low-resolution monitoring data and high-resolution memory data were used to detect collars in each dataset.

Collar Detection in Monitoring and Memory Data

We propose a 2-step algorithm as described below for detecting collars in the sensor leakage timeseries.

Design Match Filters for Detecting Collars. Due to the simultaneous vertical and rotational movement of the MFL tool in the well casing and tubing, the collar signatures in the sensor flux leakage time series vary. As showed in Figure 7(a), (b), (d) and (e), we hand labeled some collars in all sensor time series where the speed is relatively steady. We used the average of these collar labels (showed in Figure 7(c) and Figure 7(f)) as filters and applied a convolution operator over each sensor flux leakage time series to detect best matches for collars.

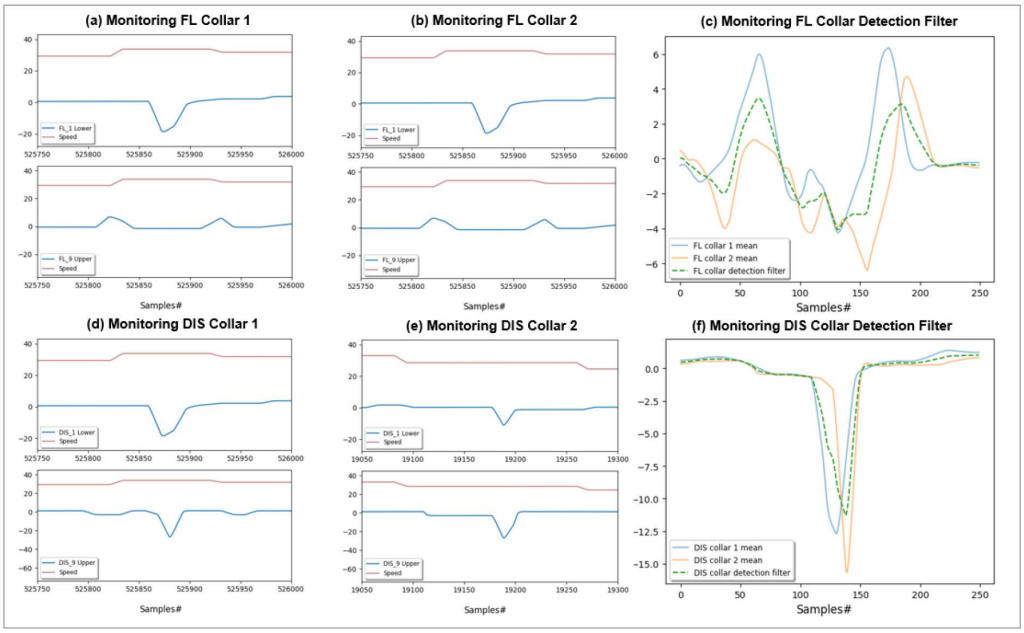

Figure 7—Create casing collar detection filter from collar signatures in tri-axial flux leakage and discriminator sensor depth series.

Figure 8(a) and Figure 7(c) shows FL and DIS sensor data along with the output from the convolution operation (labeled as matched_filter_output). Here, we can see the collar signatures (as spikes) in the FL 1 sensor aligns with the spikes in the matched filter output.

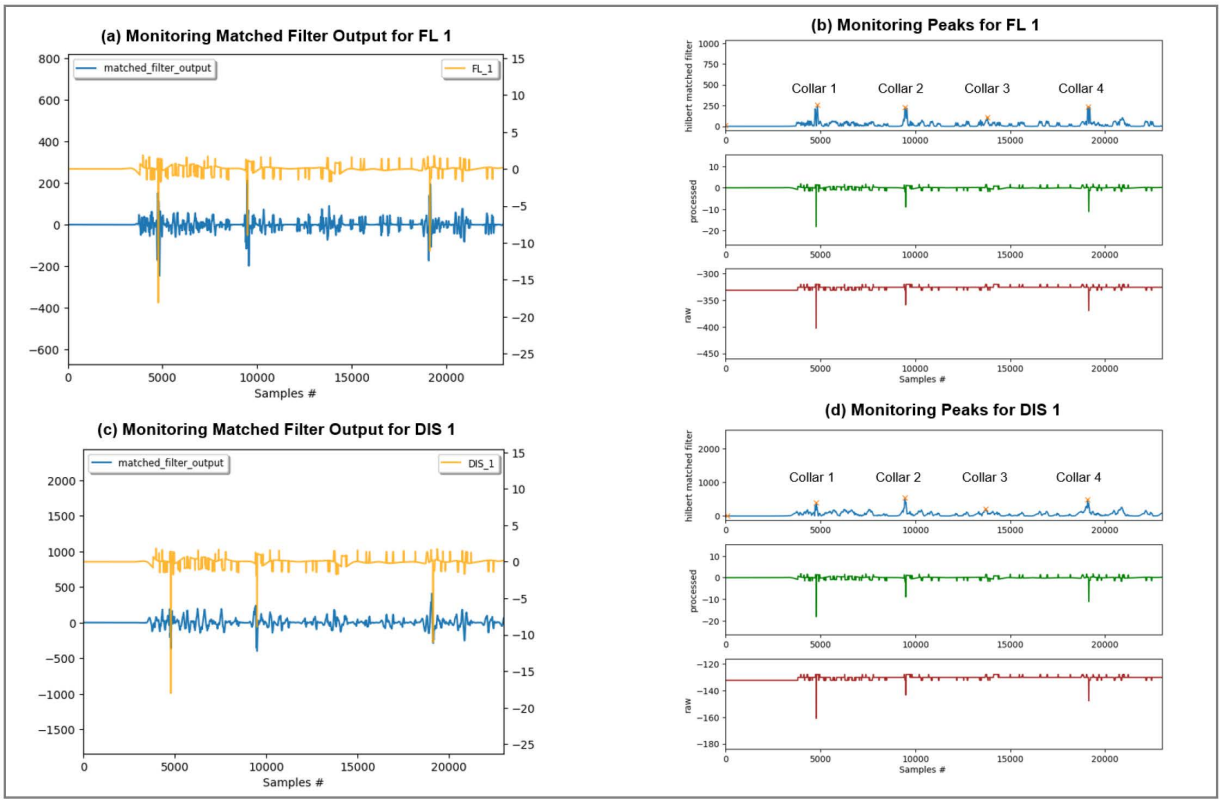

Figure 8—Detecting collars for FL 1 and DIS 1 sensor using the matched filters and pick finder.

Detect collars with Peak Finder. As the sensor flux leakage data are noisy, containing many spikes due to defects and other hardware on the casing, the matched filter output also contains many spikes. However, in the flux leakage time series, where the filter matches the best, the spikes in matched filter output are amplified. To select these amplified spikes as best candidates for collars, a pick finder function was applied on each sensor's matched filter output. The collars detected for FL 1 and DIS 1 time series are showed in Figure 8(b) and Figure 7(d). The parameters of the peak finder, such as the distance between picks, cut-off threshold for finding peaks were finetuned to match the collar distance and number of collars reported in the previous inspections or in the gamma-ray and neutron correlation log.

Average collar probability scores were generated for each of the 4 sensor groups – FL upper, FL lower, DIS upper and DIS lower, for both monitoring and memory data. Figure 9(a) show collars detected from the average collar probabilities of these 4 sensor groups in monitoring data. Figure 9 (b-e) separately show 4 sets of collars detected from these 4 sensor groups in memory data. As no speed or depth information is available in memory data, we cannot use the average of the collar probabilities from these four sensor groups for collar detection, before estimating the depth and aligning the data from these four sensor groups in memory. The next section discusses the algorithm for estimating the depth and aligning the collar probabilities of these four sensor groups in memory.

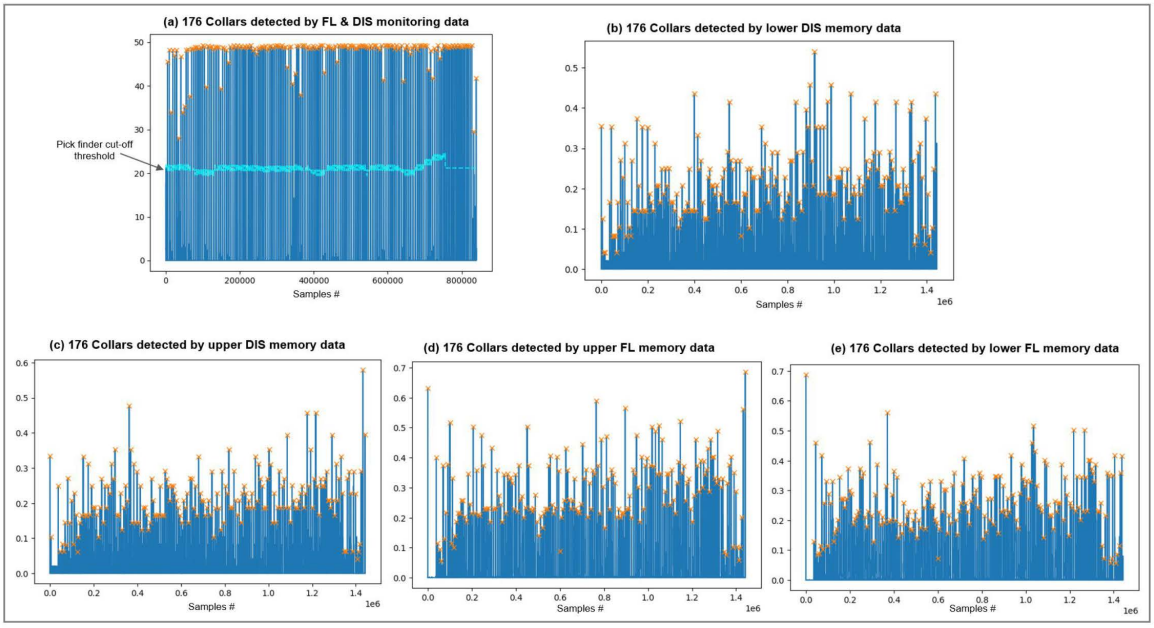

Figure 9—(a) Average collar probability with pick finder cutoff for monitoring data; (b) Average collar probability for DIS lower in memory; (c) Average collar probability for FL upper in memory; (d) Average collar probability for DIS upper in memory; (e) Average collar probability for FL lower in memory.

Collar Alignment and Depth Estimation in Memory Data

We implemented a 5-step process to estimate depth for memory data as described below.

Infer Tool Speed from Winch Speed in Monitoring Data. Though the monitoring data has lower resolution than the memory data, they both contain a "Status" filed that records time passed (in milliseconds) during the inspection log. We added the winch speed from monitoring file to the memory file using the nearest value of "Status" between these two datasets. The tool speed downhole would be closer to the winch speed that is moving the tool.

Initial Depth Estimation from Winch Speed, Monitoring Depth and Memory Accelerometer Data. Though the tool speed and depth are unknown in memory data, the time, sampling rate, and acceleration Z, Y, Z data are known. Therefore, we used Eq. (1) to estimate tool speed due to acceleration by integrating

accelerometer Z with respect to time. Accelerometer X and Y were ignored as the tool had vertical movements only. Eq. (2) calculates an initial estimation of the tool speed by adding the tool speed due to acceleration to the winch speed. As stated in Eq.3, the instantaneous displacement due to the tool speed was calculated by integrating the tool speed with respect to time. Finally, depth was estimated by subtracting this instantaneous displacement from the maximum depth found in monitoring data (as stated in Eq. (4)).

$$Tool\ Speed\ due\ to\ Accelaration = g * \int Accelerometer\ Z,\ \ where\ g = speed\ due\ to\ gravity \tag{1}$$

$$Tool\ Speed = Winch\ Speed + Tool\ Speed\ due\ to\ Accelaration \tag{2}$$

$$Displacement\ due\ to\ Tool\ Speed = \int Tool\ Speed \tag{3}$$

$$Depth = Maximum\ Monitoring\ Depth - Displacement\ due\ to\ Tool\ Speed \tag{4}$$

These equations are used in an optimization loop to improve the approximation of tool speed and depth in memory data, as described below.

Align Memory Collars. As showed in Figure 10, depth estimated in the previous step is used to align collars detected from the 4 sensor groups (FL upper, FL lower, DIS upper and DIS lower) in memory. Figure 10(a) shows the collar probabilities from 4 sensor groups, for collar # 16 – 40, over estimated depth. Here, we zoomed in on a subset of the collars to demonstrate the algorithm outputs, without making visual clutter. Figure 10(b) shows the average distance (in mm) between these collars in each group. For example, 'flu_disl_dist' refers to the average distance between collars (# 16- 40) in FL upper and DIS lower sensors, which is 2000 mm in Figure 10(b). The average distance between all collars from the 4 groups of sensors, denoted as MAE (mean absolute error) is 4437 mm. To align all the collars from the 4 sensor groups perfectly, we have to minimize the MAE to "0". We solved this as a Genetic Algorithm (GA) minimization problem. Below is the detail of how the GA minimizer was setup.

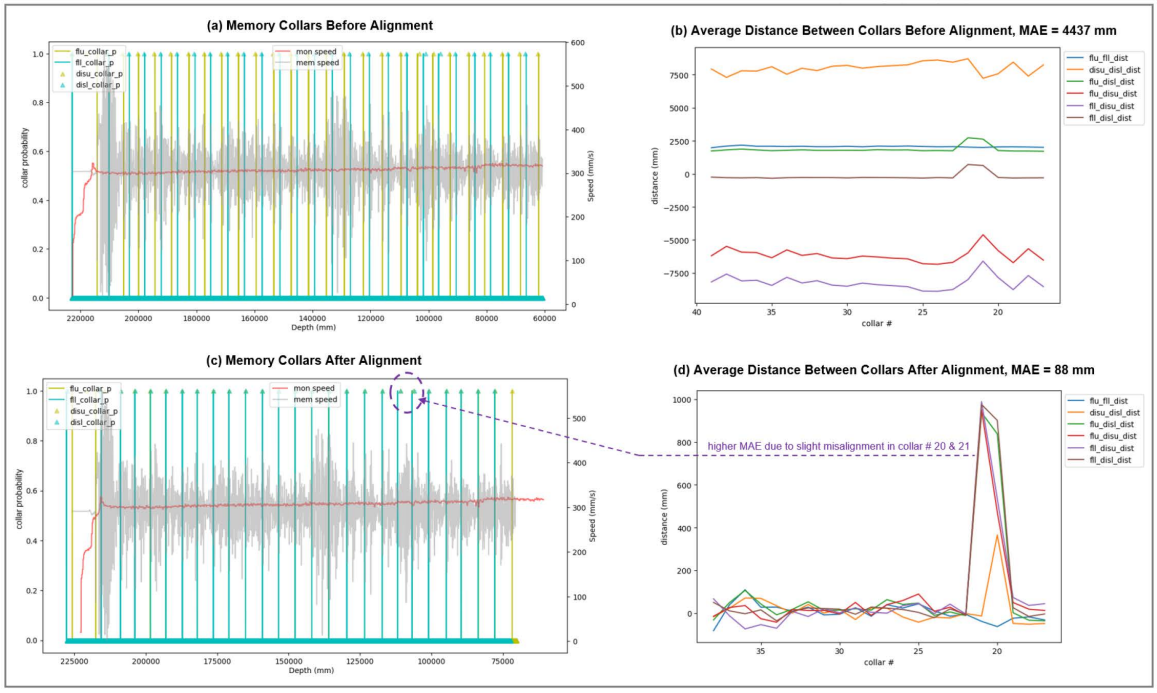

Figure 10—(a) Memory collars and winch speed over depth, before alignment; (b) MAE over memory collar number 16-40, before alignment; (c) Memory collars and winch speed over depth, after alignment; (d) MAE over memory collar number 16-40, after alignment.

GA Minimization to Align Memory Collars. The GA minimization problem was set to have MAE as its objective function and a set of 9 variables as input. GA minimizer manipulates these 9 variables to find the best solution that yield the minimum possible distance between the collars, i.e. MAE close to "0". These 9 input variables include –

1. 4 depth offsets – to account for the physical distance (mm) between FL upper, FL lower, DIS upper and DIS lower sensors
2. 4 collar offsets – to sequentially shift the collars in 4 sensor groups to the left or right in Figure 10(a), to find the best alignment as showed in Figure 10(b). Due to the physical distance between the sensors in the upper and lower module, it is possible that sensors in the upper module may miss to measure the signature of a collar downhole, as the lower module sensors have measured during an up-pass log (from the bottom hole to surface). Shifting the collars between the sensor groups helps find a better alignment when collars are missed by a sensor group, especially at the edges. i.e. at the beginning or the end of the inspection logs.
3. Tool speed – the tool speed and depth for the memory data are unknown. Eq 1–4 in section 2 is a crude approximation of these variables. Accurately approximating the tool speed would yield best alignment of collars, by accurately estimating the collar depth (as stated in Eq.4).

Upper and lower limits for the GA search space to find the best solutions for the 4 depth offsets variable were set as ± depth offsets (mm) for the 4 sensor groups from tool configuration. Search space for 4 collar offsets were set to ± 2 empirically. And the search space to find the best solution for the tool speed was set to average winch speed ± 10 (ms^{-2}). The first 2 collars and the last 2 collars were excluded from the MAE evaluation, as it is most common to have drastic speed changes at the start and the stop of the tool log, causing more misalignment in collars at the edges. Figure 10(c) shows the alignment of collar # 16-40 after using the best solution found by the GA minimizer, reducing MAE from 4437 mm to 88 mm. The figure shows that most collars were perfectly aligned. Figure 10(d) shows the MAE values for collar # 16-40. Here, we see that except collar # 20 and 21, most collars have MAE close to "0". This could be due to a sudden speed change while the MFL tool was around these collars. However, as showed in Figure 10(d), MAE for collar # 20 and 21 is less than 1000 mm or 1 m, which is within the tolerable misalignment limit for the existing methods.

Align Memory and Monitoring Collars. As monitoring depths are known, aligning the memory collars with the monitoring collars will further finetune the depth estimation of the memory collars. Accurate depth estimation of the memory collars will enable utilization of the high-resolution memory data for corrosion defects and other features detection. Therefore, we setup a second GA minimization problem with the same 9 input variables as previous section to align memory collars with monitoring collars. The objective function as was modified to include the MAE between the memory and monitoring collars, along with the MAE between the memory collars. This ensures that the GA minimization does not miss align the memory collars within themselves, as it searches for the best solution to align monitoring collars with the memory collars. The search space for the input variables were same as the GA minimization discussed in the previous step, except for the 4 depth offsets variable search space was set to ± 5000 mm empirically.

Figure 11(a) and Figure (b) shows the monitoring collars (labeled as ‘collar_loc’) in pink, along with memory collars in green and cyan, before and after the alignment with GA minimizer. Figure 11(b) shows the monitoring collars are much better aligned with memory collars after the GA minimization process. As showed in Figure(b) and (d), MAE was reduced from 1290 mm to 295 mm, which is within the tolerable alignment error limit of 1 m for the existing methods. The collars at both edges are less aligned due to rapid change in speed. Due to this reason, they were excluded from MAE calculation. The output of this step is called the "merged" data.

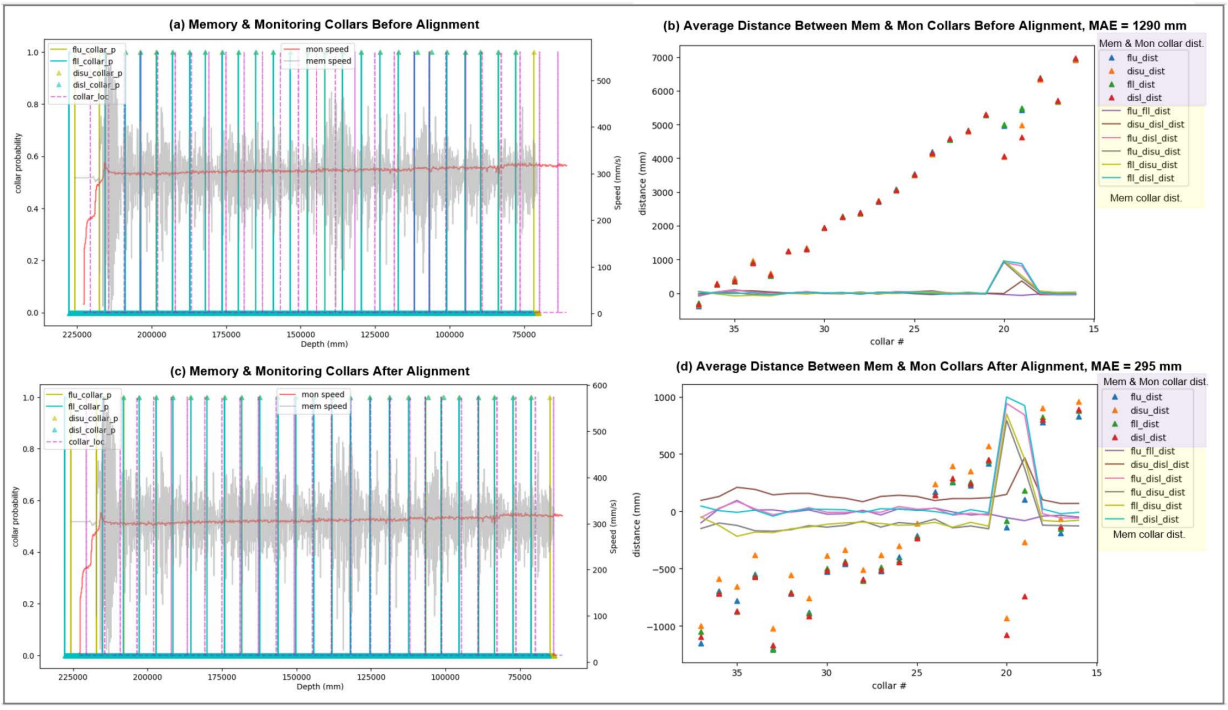

Figure 11—(a) Memory and Monitoring collars, winch speed over depth, before alignment; (b) MAE over memory collar number 16-40, before alignment; (c) Memory and Monitoring collars, winch speed over depth, after alignment; (d) MAE over memory collar number 16-40, after alignment.

Align Monitoring and Memory Collars with Collars from Previous Inspection Reports. Though monitoring collars depth are known, they don't exactly match the actual physical depth of the casing joints, and collars found in the previous inspection reports or in the gamma-ray neutron logs of the well. The experts manually correlate the collar depths in the newly created high-resolution MFL merged dataset with the previous inspection reports or in the gamma-ray neutron logs. To automate this process, we applied a third GA minimization process to align the collars in the merged dataset with the collars in the previous inspection report. The output of this step is the high-resolution MFL depth series that matches the collar depths in previous inspection reports.

Results and Conclusion

As showed in the MAE plots in 11(d), for Well 1 inspection, our algorithm outperformed the existing methods by achieving less than 50 mm misalignment between 90% of the collars in the upper and lower modules. Our algorithm also achieved reasonable alignment between 75% of the collars identified in monitoring and memory data, as well as, between previous reports and in the memory and monitoring data. However, MAE between the monitoring and memory collars show an increasing trend in Figure 11(d), instead of being random. This indicates that there's room for further improvement.

Unlike the existing manual or semi-automated methods, our proposed ML based approach can automatically identify, align and estimate depth of casing joint collars. This will significantly increase the productivity of the experts analyzing and interpreting the casing inspection data. Moreover, accurate identification of collars and accurate estimation of their location (depth) enables more accurate detection of corrosion defects in well casing.

Nomenclatures

MFL Magnetic Flux Leakage
FL Flux Leakage sensors

DIS	Discriminator sensors
flu	Flus Axial Upper
fll	Flus Axial Lower
disu	Discriminator Upper
disl	Discriminator Lower
dist	Distance
p	Probability
ms	milliseconds
mm	millimeter
m	meter
ft	feet
mon	Tool Monitoring data from MFL casing inspection
mem	Tool memory data from MFL casing inspection
GA	Genetic Algorithm
MAE	Mean Absolute Error
ML	Machine Learning
res.	resolution

References

Veanch, William D., Lloyd, Tyler S., "ID-OD Discrimination Sensor Concept for Magnetic Flux Leakage Inspection Tool," U.S. Patent 6 847 207 B1, Jan. 25, 2005.

Fickert, Gary, Haynes, John., "Oil and Gas Well Tubular Inspection System Using Hall Effect Sensors," U.S. Patent 6 924 640 B2, Aug. 2, 2005.

Vogtsberger, D. C., Girrell, B., Miller, J., D. Spencer. "Development of High-Resolution Axial Flux Leakage Casing-Inspection Tools," Paper presented at the SPE Eastern Regional Meeting, Morgantown, West Virginia, Sep. 2005. doi: https://doi.org/10.2118/97807-MS

Barolak, Joseph Gregory, Miller, Jerry E., "Apparatus and Method of Using Accelerometer Measurements for Casing Evaluations," U.S. Patent 7 595 636 B2, Sep. 29, 2009.

Brandstorm, Randel, "Apparatus and Method for Detection of Defects Using Flux Leakage Techniques," U.S. Patent 7 804 295 B2, Sep. 28, 2010.

El Sherbeny, Wael, Nuic, Ivo, Hasan, Gasser, Abdesslam, Abba, Tharwat Hassane., "Magnetic Flux Leakage (MFL) Technology Provides the Industry's Most Precise Pipe Integrity and Corrosion Evaluation, Accurately Characterizing Casing and Tubing Strength. Technology Overview and Case History." Paper presented at the SPE North Africa Technical Conference and Exhibition, Cairo, Egypt, Sep. 2015. doi: https://doi.org/10.2118/175871-MS

Foster, R. L., D. Jacobson., "A Wireline Logging Method for the Orientation of Fiber Optic and Control Lines in Highly Deviated or Horizontal Well Sections," Paper presented at the SPE Eastern Regional Meeting, Morgantown, West Virginia, USA, Oct. 2015. doi: https://doi.org/10.2118/177307-MS